BIOCHEMISTRY
including biophysical chemistry & molecular biology

Article

pubs.acs.org/biochemistry

Lactose Repressor Experimental Folding Landscape: Fundamental Functional Unit and Tetramer Folding Mechanisms

Roee Ramot,[†] Krishna Kishore Inampudi,[†] and Corey J. Wilson*[,†,‡]

[†]Department of Chemical and Environmental Engineering, Yale University, New Haven, Connecticut 06511, United States
[‡]Department of Molecular Biophysics and Biochemistry, Yale University, New Haven, Connecticut 06511, United States

Supporting Information

ABSTRACT: The fundamental principles that govern monomer folding are believed to be congruent with those of protein oligomers. However, the effects of protein assembly during the folding reaction can result in a series of complex transitions that are considerably more challenging to deconvolute. Here we developed the experimental protein folding mechanism for the lactose repressor (LacI), for both the dimeric and the tetrameric states, using equilibrium unfolding and kinetic experiments, and by leveraging the previously reported monomer folding landscape. Reaction details for LacI oligomers were observed by way of circular dichroism, intrinsic fluorescence, and Förster resonance energy transfer (FRET) and as a function of protein concentration. In general, the dimer and tetramer are four-phase folding reactions in which the first three transitions are tantamount to the folding of constituent monomers. The final reaction phase of the LacI dimer can be attributed to protein assembly, based on the concentration dependence of the observed folding rates and intermolecular FRET measurements. Unlike the dimer, the latter reaction phase of the LacI tetramer is not dependent on protein concentration, likely because of a strong tethering of the monomers, which simplifies the folding reaction by eliminating an explicit protein assembly phase. Finally, folding of the LacI dimer and tetramer was assessed in the presence of polyethylene glycol to rule out inert molecular crowding as the driving force for the protein folding reaction; in addition, these data provide insight into the folding mechanism in vivo.

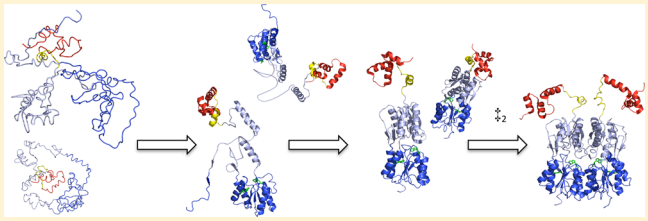

The ability to form dimeric or higher-order oligomers dramatically enhances the biological activity of many proteins.[1] This is of crucial importance for DNA binding proteins. In prokaryotes, such proteins need to be able to recognize a sequence that is at least 11−12 bp long if the target site is to occur in a genome only once or a few times.[2,3] However, a typical helix−turn−helix recognition motif and other structural classes of DNA recognition motifs (e.g., zinc finger,[4] zipper motifs,[5] and β-hairpin [6]) is capable of interacting only with a maximum of 5−6 bp, because of geometric constraints, although the exact constraints for other motifs may vary some.[7,8] Therefore, the ability to form dimers (or higher-order multimers) is of paramount importance. Thus, understanding and predicting the determinants of assembly are clearly important; undoubtedly, this will require a thorough understanding of the folding reaction of protein oligomers. Although the physicochemical properties identified for monomer folding also apply to the folding of dimeric proteins, the effects of protein−protein association during the folding reaction can manifest in complex ways, ranging from a two-state transition involving a native dimer and denatured monomers to mechanisms that involve one or more monomeric or dimeric intermediate states.[9] To date, a relatively small number of folding studies of protein oligomers have been conducted. To illuminate our understanding of the protein folding and assembly relationship, here we present an experimentally derived folding mechanism for the lactose repressor (LacI), i.e., in dimeric and tetrameric forms.

LacI is a well-studied negative gene regulator. This prototypic repressor is an example of a protein system in which assembly is required for activity.[10] The LacI structure is best described as a dimer of dimers, and each protein monomer can be decomposed into five structural units (Figure 1). Concisely, a given monomer has an N-terminal helix−turn−helix motif (residues 1−61), comprising the DNA binding domain and a monomer core (residues 62−330) that is divided into N- and C-subdomains with three crossovers between the two regions such that the cleft between the two subdomains forms the effector binding site. The monomer−monomer interface that confers dimer assembly is confined to the C-subdomain, whereas the N-subdomain serves as the mediator for allosteric communication between the effector binding site and the DNA binding domain. The fundamental functional unit of LacI is a dimer; that is, the dimer is regarded as the minimal state needed to produce the basic modulated DNA binding function. In nature, LacI exists as a tetramer for which the assembly of two functional units is accomplished by way of a tetramerization domain (residues 331−360). Functionally, the LacI

Received: April 27, 2012
Revised: August 9, 2012
Published: August 29, 2012

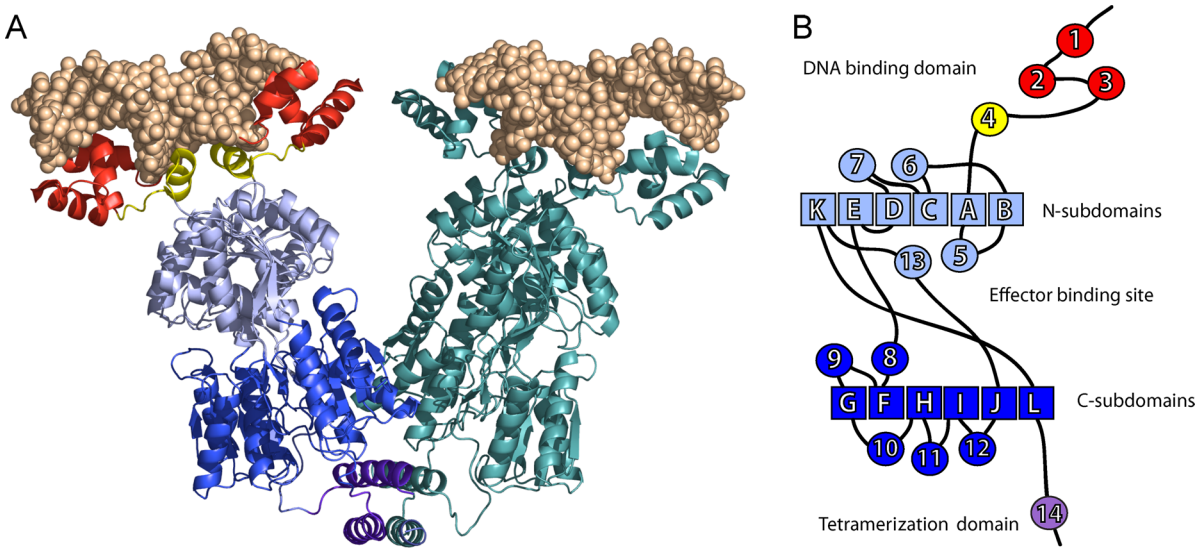

Figure 1. Lactose repressor (LacI) structure and topology. (A) The LacI tetramer consists of the following structural units: N-subdomain (light blue), C-subdomain (dark blue), DNA binding domain (red and yellow), tetramerization domain (purple), and operator DNA (light brown). The effector binding site is located between the N- and C-subdomains. LacI (tetramer) has a molecular mass of 150 kDa; each monomer is 360 amino acids in length. The structure is given in the repressed state, i.e., without the inducer analogue IPTG. (B) Topological cartoon of a LacI monomer, in which circles and squares represent α-helices and β-sheets, respectively.

tetramer enhances gene suppression via the formation of repression loops.[11]

To date, a thorough understanding of the LacI monomer folding mechanism was achieved by way of a concerted experimental and computational effort.[12,13] These studies revealed a three-phase folding mechanism:

$$U \xrightarrow{k_{burst}} I_b \xrightarrow{k_1} I \xrightarrow{k_2} N$$

Namely, the refolding reaction is initiated by the formation of a burst-phase intermediate (I_b) that rearranges to form an on-pathway intermediate (I) that consists of a partially folded C-subdomain and an unfolded N-subdomain, which leads to the native state (N). In contrast, only a fundamental assessment of the LacI dimer and tetramer unfolding (under equilibrium conditions) has been reported.[14,15] In the study presented here, we established an experimentally derived folding mechanism for both the LacI dimer and the tetramer that builds on the established folding landscape for the LacI monomer.[12] By employing four complementary reaction coordinates [i.e., circular dichroism (CD), fluorescence, intermolecular Förster resonance energy transfer (FRET), and protein concentration], we were able to deconvolute critical reaction phases for both the folding and coupled assembly reactions. In addition, we investigated the folding mechanism of LacI in the presence of a molecular crowding agent (i) to rule out inert crowding as the cause of the observed changes in unfolding and folding rates and (ii) to gain insight into the putative in vivo folding mechanism. On the basis of this collection of data, we propose two distinguishing mechanisms for the LacI dimer and tetramer that expand our understanding of the complex folding–assembly landscape of a prototypic regulatory element.

MATERIALS AND METHODS

Protein Expression, Purification, and Hydrodynamics. The expression vectors for both the LacI dimer and tetramer are derivatives of the pJC1 LacI construct.[16] The LacI dimer was produced via the introduction of a premature C-terminal stop codon to delete 11 C-terminal residues from the tetramerization domain.[16,17] LacI proteins were expressed in BL26 blue *Escherichia coli* cells (Novagen) that were cured of the episome carrying the I^q promoter and the *lacI* gene. Purification was conducted using the protocol outlined in the Supporting Information. The protein concentration was determined using the extinction coefficient for wild-type LacI (ε_{280} = 0.6 mL mg^{-1} cm^{-1}) and a Bradford assay (Bio-Rad) or a Lowry assay.[18] Purified proteins were >99% pure according to sodium dodecyl sulfate gel electrophoresis. The hydrodynamic radii of the LacI dimer and tetramer were assessed as a function of protein concentration by way of analytical molecular sieve chromatography using a Superdex 200 10/300GL analytical column. The column was equilibrated with 100 mM potassium phosphate (pH 7.5) and calibrated with ribonuclease A (13.7 kDa), chymotrypsinogen A (25.0 kDa), ovalbumin (43.0 kDa), bovine serum albumin (67.0 kDa), and blue dextran 200 (2000 kDa). LacI dimer and monomer variants were eluted from the column at protein concentrations ranging from 0.3 to 30.0 μM.

Equilibrium Unfolding and Analysis. Equilibrium unfolding of the LacI dimer and tetramer was conducted using the protocol established by Wittung-Stafshede et al.[12] Equilibrium unfolding of a given protein was monitored by far-UV CD at 222 nm and by way of intrinsic tryptophan fluorescence (λ_{ex} = 285 nm) using an Applied Photophysics (Leatherhead, U.K.) spectrometer. The protein concentration was varied between 0.3 and 3.0 μM, such that at least three independent isothermal experiments were conducted as a function of urea concentration at a given protein concentration. The protein concentration range was determined by the detection limits (0.3 μM lower limit) and kinetic refolding limit for aggregation (3.0 μM). These limits are additionally applied in the experiments listed in Protein Folding–Assembly Dynamics. Nonlinear least squares was used to directly fit primary data; i.e., equilibrium unfolding isotherms were fit to a two-state model.[19] The ellipticity is reported as the mean residue molar ellipticity ([θ] in degrees square centimeters per decimole). The primary circular dichroism signal (millidegrees)

dx.doi.org/10.1021/bi300545f | *Biochemistry* 2012, 51, 7569–7579

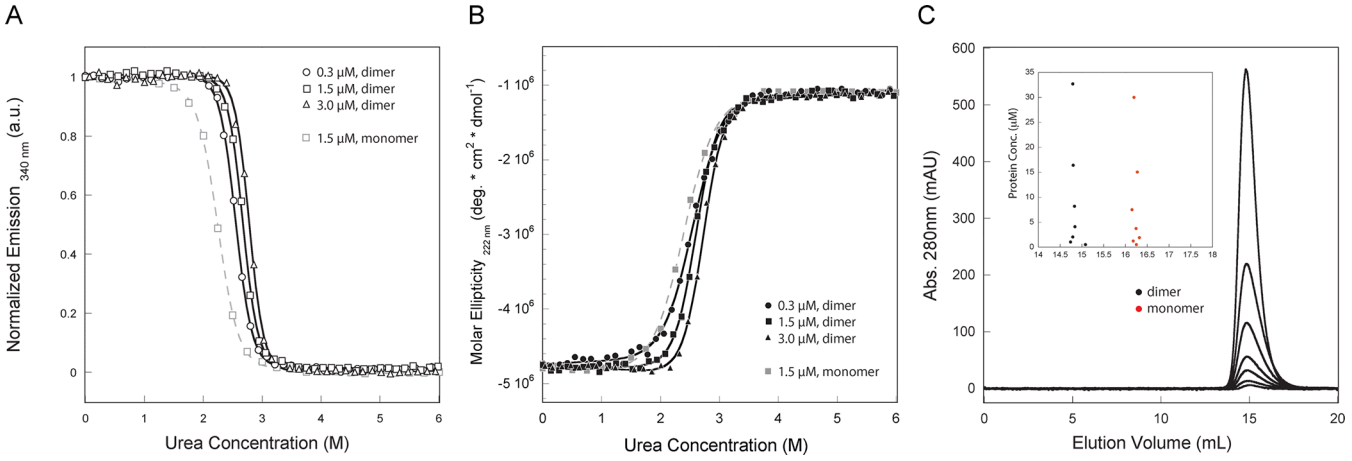

Figure 2. Thermodynamic characterization of the LacI dimer. (A and B) Equilibrium unfolding of the LacI dimer as a function of urea and protein concentration [0.3 μM (circles), 1.5 μM (squares), and 3.0 μM (triangles)] observed by (A) fluorescence emission at 340 nm (empty symbols) and (B) far-UV CD at 222 nm (filled symbols). The equilibrium unfolding profile for the LacI monomer is colored gray. The solid lines (and dashed gray lines) represent individual fits to a two-state denaturant model; a summary of the data is given in Table 1. (C) Assessment of the oligomeric state of the LacI dimer as a function of protein concentration, ranging from 30.0 to 0.3 μM. The inset shows hydrodynamic peak maxima of (i) the refolded dimer (black dots) and (ii) the monomer (red dots).

was transformed using the procedure described in ref 16. Standard deviations presented in Tables 1−3 were derived from three or more independent experiments.

Protein Folding−Assembly Dynamics. Time-resolved folding, unfolding, and interaction measurements were taken on an Applied Photophysics Chirascan stopped-flow reaction analyzer in fluorescence (λ_{ex} = 285 nm and monitored λ_{em} = 340 nm) and CD (monitored λ_{abs} = 222 nm) modes. The buffer was 100 mM potassium phosphate (pH 7.5) at 20 °C. The LacI dimer (or tetramer) was mixed at a 1:5 ratio with appropriate urea buffer solutions to trigger refolding or unfolding. Under each condition, a minimum of six kinetic traces were averaged and fit to monophasic (unfolding) and biphasic or triphasic decay (refolding) equations using a nonlinear least-squares algorithm, with software supplied by Applied Photophysics (also see the Supporting Information). The refolding rate constants k_{f1} and k_{f2} as a function of urea concentration were fit as a linear dependence with urea.[20] The unfolding k_u and latter refolding k_{f3} rate constants at different urea concentrations were fit assuming nonlinear urea dependence by way of a set of second-order polynomials.[21,22] In all cases, the protein (monomer) concentration was varied between 0.3 and 3.0 μM. Protein concentrations lower than 0.3 μM could not be detected reliably via CD kinetics. In addition, protein concentrations much higher than 3.0 μM that converged on the stopped-flow observation cell resulted in aggregation. A LacI protein concentration of ≤3.0 μM could be kinetically refolded with >98% recovery (also see Figure S2 and Table S1 of the Supporting Information). Polyethylene glycol 1500 (SpectauM) was used as a molecular crowding agent at 6 and 12% (w/v), for both kinetic and equilibrium experiments. Standard deviations presented in Tables 1−3 were derived from three or more independent experiments.

Time-Resolved LacI Association and Dissociation by Way of Intermolecular Förster Resonance Energy Transfer (FRET). Singly labeled protein was prepared using a standard labeling protocol with either the Oregon-Green 488 maleimide (donor) or the Texas-Red maleimide (acceptor) chromophore (Invitrogen, Carlsbad, CA). The LacI dimer containing engineered cysteine residues at solvent-exposed positions 207 and 227 (located in the C-subdomain) was incubated in 150 mg/L DTT [buffered at 0.03 M KPO_4 (pH 7.5) and 5% glucose] for at least 30 min. DTT was removed via a GE HiTrap 5 mL desalting column. Proteins were maintained in an oxygen-free and low-light environment throughout the labeling procedure. Stock solutions of protein were prepared in 5% dimethyl sulfoxide (DMSO) to improve labeling efficiency. Labeling was verified using gel filtration (Superdex 200 10/300GL column); accordingly, protein after gel filtration was used in the experiments described in this study to eliminate or reduce DMSO contamination. Note, unmodified proteins (i.e., without introduced point-mutated cysteine) did not yield (detectable) labeled LacI. The protein concentration was determined by way of a Bradford Assay (Bio-Rad) or a Lowry assay,[18] relative to a wild-type LacI dimer standard curve. To estimate the quality of the point-mutated LacI proteins, stability and folding dynamics of unlabeled thiol derivatives were measured. In all cases, extrapolated values were within the standard deviation of the wild-type dimer measurements. Label proteins were mixed at 1:20 molar ratios with unlabeled proteins. Intermolecular FRET measurements were conducted using a rapid-mixing strategy using an Applied Photophysics spectrometer equipped with a stopped-flow accessory. The donor λ_{ex} = 495 nm, and the reaction was monitored via acceptor λ_{em} = 610 nm, with complementary observation given by donor λ_{em} = 514 nm decay. Intermolecular association and dissociation were assessed as a function of urea and protein concentration at a 1:3 donor:acceptor ratio. Measurements were taken with two independent distances, 4 and 7 nm, accommodated using labels at position R207C or Q227C. Extrapolated measurements are based on at least three independent experiments, and reported data are based on average values (Tables 1 and 3).

RESULTS AND DISCUSSION

Equilibrium Unfolding of the LacI Dimer. Figure 2 is a set of equilibrium unfolding reaction profiles of the LacI dimer, using the chemical denaturant urea. Isothermal unfolding occurs as a single cooperative transition, observed by way of intrinsic tryptophan fluorescence and far-UV CD. Both modes

dx.doi.org/10.1021/bi300545f | Biochemistry 2012, 51, 7569−7579

Table 1. Equilibrium Unfolding and Dynamics of Unfolding and Folding of the LacI Dimer as a Function of Urea and Protein Concentration[a]

	LacI dimer (0.3 μM)		LacI dimer (1.5 μM)		LacI dimer (3.0 μM)	
	fluorescence	far-UV CD	fluorescence	far-UV CD	fluorescence	far-UV CD
ΔG_{eq} (kJ mol^{-1})	43.0 ± 1.2	30.0 ± 1.3	48.0 ± 1.1	40.0 ± 1.4	50.0 ± 1.2	46.0 ± 1.5
m_{eq} (kJ mol^{-1} M^{-1})	17.0 ± 1.1	12.2 ± 1.0	18.6 ± 1.2	15.5 ± 1.2	18.5 ± 1.1	17.2 ± 1.1
$[urea]_{1/2eq}$ (M)	2.5 ± 0.1	2.5 ± 0.2	2.6 ± 0.1	2.6 ± 0.2	2.7 ± 0.1	2.7 ± 0.1
k_{burst} (s^{-1})	>1000	–	>1000	>1000	>1000	>1000
k_{f1} (s^{-1})	0.36 ± 0.02	–	0.33 ± 0.01	0.31 ± 0.04	0.33 ± 0.01	0.34 ± 0.02
k_{f2} (s^{-1})	0.056 ± 0.003	–	0.060 ± 0.002	0.058 ± 0.003	0.058 ± 0.001	0.061 ± 0.002
k_{f3} (s^{-1})	0.0041 ± 0.0002	–	0.0056 ± 0.0002	–	0.0081 ± 0.0002	–
k_u (s^{-1})	(1.7 ± 0.1) ×10^{-8}	–	(1.0 ± 0.1) × 10^{-8}	(8.5 ± 0.1) × 10^{-9}	(6.7 ± 0.5) × 10^{-9}	(5.7 ± 0.5) × 10^{-9}
k_{f_FRET} (s^{-1})	0.0065 ± 0.0001	–	0.0097 ± 0.0001	–	0.014 ± 0.0001	–
k_{u_FRET} (s^{-1})	0.0034 ± 0.002	–	0.0021 ± 0.001	–	0.016 ± 0.001	–

[a]Standard deviations are based on three or more independent experiments. A low signal:noise ratio at 0.3 μM for CD prevented the collection of reliable kinetic data.

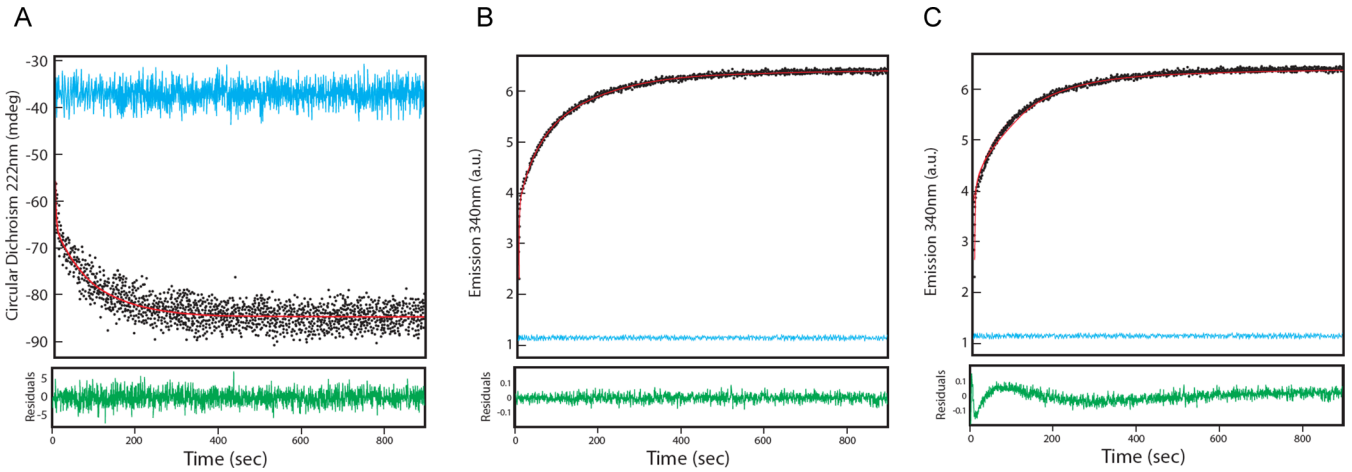

Figure 3. Relaxation curves (refolding kinetics) for the LacI dimer. Representative kinetic refolding traces observed by far-UV CD at 222 nm (A) and intrinsic fluorescence at a λ_{em} of 340 nm (B and C). Blue and black data points indicate the unfolded baseline and observed refolding signal, respectively. Fits of the primary data are colored red, i.e., to a (i) biphasic (A and C) or (ii) triphasic (B) reaction model. The residuals for each fit are given below each kinetic trace (green). The amplitudes for refolding observed by intrinsic fluorescence are k_{burst_FL} (20%), k_{f1_FL} (30%), k_{f2_FL} (40%), and k_{f3_FL} (10%), whereas refolding amplitudes observed via CD are k_{burst_CD} (40%), k_{f1_CD} (10%), and k_{f2_CD} (50%).

of detection show a single unfolding transition that is dependent on protein concentration over the range tested. Both observables show a definitive shift in the unfolding midpoint to a higher denaturant concentration as the LacI protein concentration increases. Nonlinear least-squares fitting of the primary data was conducted, where two-state behavior was assumed. Isothermal data for each concentration were evaluated individually, and the corresponding analysis is summarized in Table 1. Fluorescence and CD data are described well by the two-state model[19,23] at a given protein concentration, and the unfolding midpoints are nearly coincidental. Table 1 reveals a general increase in m_{eq} and ΔG_{eq} with an increase in protein concentration. In addition, the extrapolated stabilities and m values observed by fluorescence and CD at a given protein concentration are divergent. That is, the global secondary structure unfolding (CD, measured at 222 nm) is less cooperative than the local fluorescence measurements. At the lowest measured protein concentration, the LacI dimer has a stability observed via CD that is on par with that of the LacI monomer.[12] An assessment of refolded dimer hydrodynamics at variable protein concentrations revealed a small shift to a larger than to a smaller radius at the two lowest protein concentrations (Figure 2C), which is in agreement with a native protein not exposed to urea. The lowest observed dimeric protein concentration (~0.3 μM) elutes with a hydrodynamic radius that is slightly smaller than that at higher dimer concentrations. Accordingly, these data suggest a dynamic equilibrium between the dimer and monomer species, where the homodimer has an apparent K_d of <300 nM (Figure 2C). The differences in m_{eq} and ΔG_{eq} for a given protein concentration suggest that a simple two-state unfolding model cannot adequately describe the LacI dimer isothermal unfolding data. Qualitatively, the isothermal data are consistent with a multistate mechanism; that is, variation in m_{eq} with protein concentration is indicative of a populated intermediate under equilibrium conditions.[24] Moreover, an increase in both m_{eq} and ΔG_{eq} is consistent with a dimer unfolding via a three-state denaturation model involving a monomeric intermediate.[25] In the simplest case, the increase in m_{eq} with protein concentration can be explained by dissociation of the dimer in the transition region at low protein concentrations;[25−27] in all cases, our analysis of equilibrium data will provide only a limited view of the unfolding mechanism. Accordingly, we performed kinetic studies observed using circular dichroism (CD), intrinsic fluorescence, and Förster resonance energy transfer (FRET), as a function of protein concentration, and in the presence of

dx.doi.org/10.1021/bi300545f | Biochemistry 2012, 51, 7569−7579

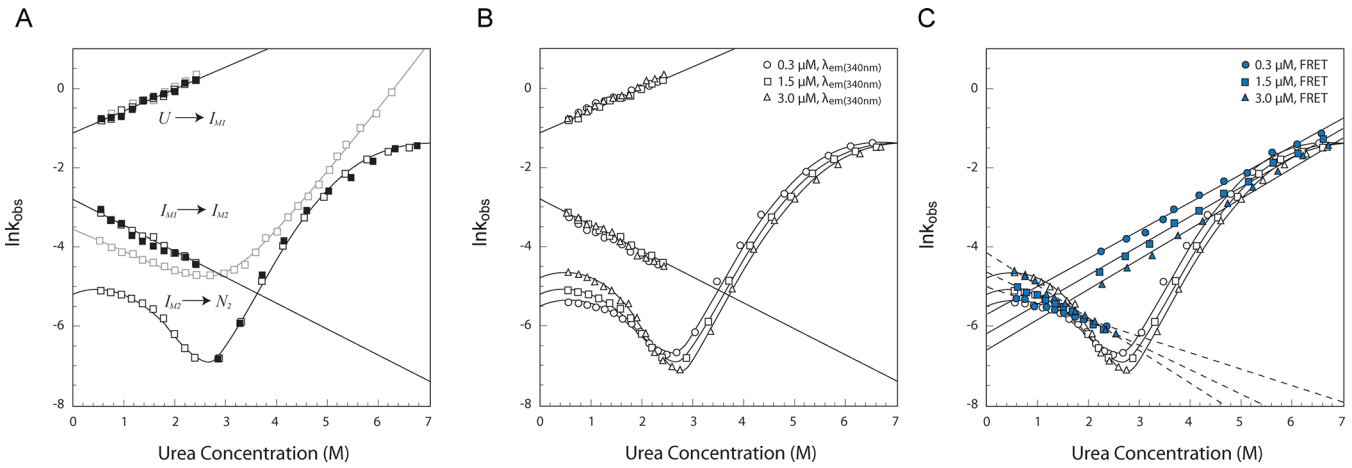

Figure 4. Assessment of LacI dimer folding dynamics. (A) Semilogarithmic plot of the observed rate as a function of urea concentration, monitored by CD (filled symbols) and fluorescence (empty symbols). Monomeric LacI reaction kinetics are colored gray. (B) Observed refolding and unfolding reactions as a function of protein concentration [0.3 μM (circles), 1.5 μM (squares), and 3.0 μM (triangles)] observed by fluorescence. The corresponding CD profiles are shown in Figure S1 of the Supporting Information. (C) LacI dimer dissociation and association kinetics as a function of urea and protein concentration during the unfolding and refolding reactions, respectively, monitored by intermolecular FRET (blue symbols). FRET data were overlaid on corresponding fluorescence data (empty symbols).

polyethylene glycol (PEG) to better elucidate the preferred unfolding and folding routes.

LacI Dimer Folding Dynamics. To improve our understanding of the folding mechanism of the LacI dimer, kinetic folding studies were performed. Time-resolved unfolding and refolding experiments were conducted via stopped-flow mixing techniques using variable urea concentrations, monitored by far-UV CD and intrinsic protein (tryptophan) fluorescence. The observed dynamic unfolding of the LacI dimer at a given urea concentration is best fit to a first-order reaction model with a single exponential for both modes of detection. All unfolding kinetic traces are devoid of missing amplitudes. In contrast, the refolding reaction for the dimer is a multistate process composed of four kinetic phases observed via fluorescence and three distinct CD phases, such that both observables include a burst phase (Figure 3). The denaturant concentration dependence of LacI unfolding and refolding was examined to obtain rate constants in the absence of denaturant (Figure 4A). The lone unfolding arm (3−7 M urea) presence as a nonlinear correlation for both modes of detection, whereas the refolding reaction (0−3 M urea) consists of three observable phases, excluding the burst-phase reaction. The fastest observable refolding phase (k_{f1}) exhibits a linear correlation with a positive slope with an increase in the concentration of the chemical denaturant. The logarithm of the rate constant for the interim refolding phase (k_{f2}) exhibits a canonical linear dependence with a negative slope. Finally, the slowest kinetic phase (k_{f3}) reveals a nonlinear urea dependence; this process is observed only via fluorescence. The amplitude percentages are shown in Figure S1 of the Supporting Information.

An assessment of the observed refolding and unfolding reactions was conducted over a 10-fold range of protein concentrations (Figure 4B). The extrapolated rate of the unfolding reaction decreases with a corresponding increase in protein concentration, for both CD (see Figure S1 of the Supporting Information) and fluorescence measurements. Likewise, the latter-phase fluorescence (k_{f3}) refolding exhibits a protein concentration dependence accompanied by distinctive curvature in the folding arm, such that the rate increases with an increase in protein concentration. All other refolding rate constants appear to be independent of protein concentration. The results of this assessment are summarized in Table 1.

Developing the Folding Mechanism for the LacI Dimer. To construct a LacI dimer folding mechanism based on the folding experiments presented here, we leveraged a thorough understanding of the folding landscape of the LacI monomer developed in an earlier study.[12,13] The most salient differences between the monomeric and dimeric folding landscapes involve additional refolding phase and distinctive curvature in the unfolding and the latter refolding arms (Figure 4). The downward curvature in plots of the observed (un)folding rate as a function of denaturant concentration can be attributed to various causes.[9,28−30] The most reasonable supposition is that the curvature observed here in the refolding arm (0−3 M urea) and unfolding arm (3−7 M urea) is the result of protein association and dissociation, respectively. This deduction is increasingly evident upon examination of the LacI concentration dependence of the observed rates (Figure 4B). However, to rule out aggregation (misfolding) as a contributor to the nonlinear urea dependence, the refolded protein was isolated and re-evaluated for structure and function. Analysis of the refolded dimer revealed hydrodynamics and CD spectra nearly identical to those of the folded protein. Isothermal titration calorimetry (ITC) indicates that the refolded protein retains nativelike affinity for the substrate analogue IPTG (Figure S2 of the Supporting Information). Taken together, these data suggest that the LacI dimer folds reversibly, devoid of aggregation, under the conditions tested.

To explicitly assign LacI assembly and dissociation to the refolding and unfolding reactions, respectively, we conducted time-resolved intermolecular FRET experiments at variable urea and protein concentrations (Figure 4C). The rate constant for dimer dissociation correlates with the linear extrapolation of the microscopic folding rates at higher denaturant concentrations (5−7 M urea). Accordingly, the rate of LacI dissociation decreases with an increase in the protein concentration (data summarized in Table 1). In other words, the rate of monomer association effectively competes with the rate of monomer unfolding, reducing the overall speed at which

dx.doi.org/10.1021/bi300545f | Biochemistry 2012, 51, 7569−7579

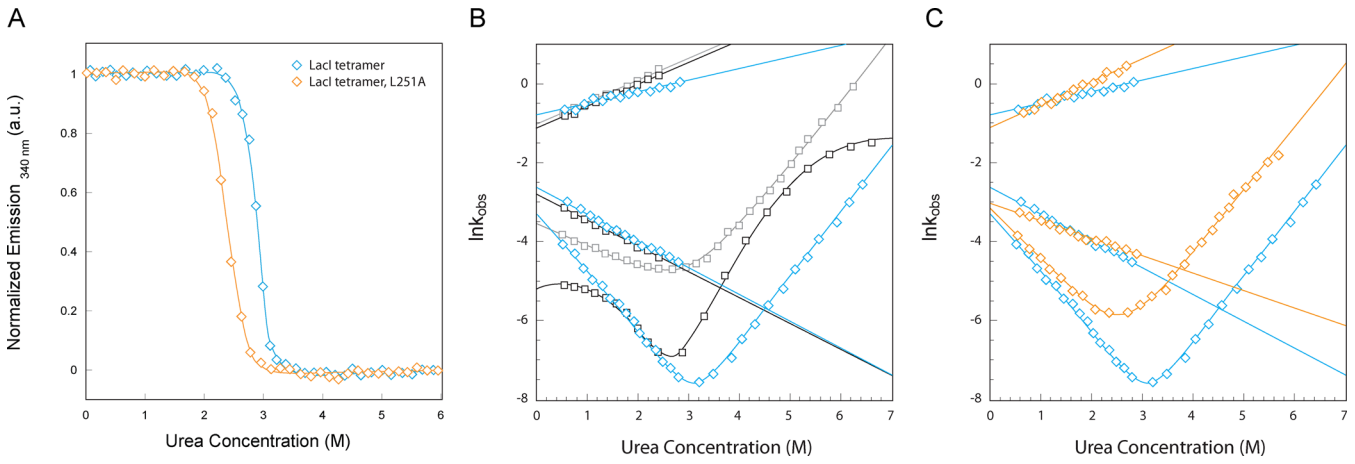

Figure 5. Equilibrium unfolding and kinetic assessment of the LacI tetramer and L251A tetramer. (A) Equilibrium unfolding of the LacI tetramer (empty blue diamonds) and the L251A LacI tetramer (empty orange diamonds) using the chemical denaturant urea, observed by fluorescence. (B) Semilogarithmic plot of the observed (intrinsic fluorescence λ_{em} = 340 nm) unfolding and folding rates of the LacI tetramer (empty blue diamonds) as a function of urea concentration, relative to LacI monomer (empty gray squares) and LacI dimer (empty black squares). (C) Kinetic assessment of the L251A LacI tetramer (empty orange diamonds) by fluorescence, relative to the LacI tetramer (empty blue diamonds).

Table 2. Equilibrium Unfolding and Dynamics of Unfolding and Folding of the LacI Tetramer[a]

	LacI tetramer		LacI tetramer (L251A)	
	fluorescence	far-UV CD	fluorescence	far-UV CD
ΔG_{eq} (kJ mol^{-1})	65.6 ± 1.5	65.5 ± 2.0	38.8 ± 1.5	39.1 ± 2.0
m_{eq} (kJ mol^{-1} M^{-1})	22.6 ± 1.0	22.9 ± 2.0	16.1 ± 1.2	16.3 ± 1.5
$[urea]_{1/2eq}$ (M)	2.9 ± 0.1	2.9 ± 0.2	2.4 ± 0.1	2.4 ± 0.2
k_{burst} (s^{-1})	>1000	>1000	>1000	>1000
k_{f1} (s^{-1})	0.450 ± 0.01	0.430 ± 0.01	0.35 ± 0.02	0.34 ± 0.02
k_{f2} (s^{-1})	0.074 ± 0.002	0.072 ± 0.001	0.050 ± 0.001	0.051 ± 0.002
k_{f3} (s^{-1})	0.037 ± 0.001	–	0.041 ± 0.001	–
k_u (s^{-1})	(6.1 ± 0.1) × 10^{-9}	(5.79 ± 0.1) × 10^{-9}	(1.2 ± 0.1) × 10^{-4}	(1.0 ± 0.1) × 10^{-4}
k_{f_FRET} (s^{-1})	–	–	–	–
k_{u_FRET} (s^{-1})	–	–	–	–

[a]Standard deviations are based on three or more independent experiments. Explicit assembly and dissociation during the refolding and unfolding reactions, respectively, could not be observed by FRET experiments because of the strong interaction conferred by the tetramerization domain.

the dimer becomes completely unfolded. Under refolding conditions, the rate constant for dimer association is concurrent with the latter reaction phase. Hence, the rate of assembly during the folding reaction increases with protein concentration and is concomitant with the refolding reaction at lower denaturant concentrations. On the basis of the experiments presented in this study (in addition to details with regard to the monomer folding landscape), the putative folding mechanism for the LacI dimer is as follows (also see Figure 4A):

$$U \xrightarrow{k_{burst}} I_b \xrightarrow{k_1} I_{M1} \xrightarrow{k_2} I_{M2} \xrightarrow{k_3^{\ddagger_2}} N_2$$

The folding reaction is initiated by a burst-phase intermediate (I_{burst}), which forms within the dead time of the stopped flow. Subsequently, I_{burst} rearranges on a measurable time scale to form a second (on-pathway) intermediate (I_{M1}) that is rate-limited by an unfolding event. Thus far, the dimeric folding reaction is consistent with the monomeric LacI folding mechanism, published previously.[12,13] The completion of monomer folding by way of a second monomeric intermediate (I_{M2}) precedes the assembly reaction; i.e., the protein−protein interaction is rate-limited by I_{M2} formation. The putative bimolecular transition state can form only once the C-subdomain has been completely structured, which requires a well-ordered N-subdomain because of topological constraints (Figure 1); namely, interface helices 10−12 achieve a nativelike configuration only once helix 13 and β-sheet K have formed in the N-subdomain. Accordingly, the protein−protein binding transition state ($\ddagger_2$) is synonymous with the formation of a bimolecular native state (N_2).

LacI Tetramer Folding Landscape. The LacI tetramer unfolding under equilibrium conditions is an apparent two-state reaction (Figure 5A), in which unfolding isotherms observed by intrinsic tryptophan fluorescence and CD are coincidental (data summarized in Table 2). Tetramer unfolding is independent of protein concentration, with an unfolding midpoint at 2.9 M urea and an ~ΔG_{eq} of 66 kJ mol^{-1} over a 10-fold increase in protein concentration. Thus far, all equilibrium observations are consistent with earlier reports.[14] The time-resolved unfolding measurements for the tetramer are observed as single-phase kinetics in both modes of detection, whereas in the refolding process, the observed relaxation to the native state exhibits distinct three- and four-phase behavior (including a burst phase) when probed by CD and fluorescence, respectively, i.e., with amplitudes similar to those reported for the dimer. Figure 5B is an assessment of the logarithm of the observed rates as a function of denaturant concentration. The unfolding event is observed as a single linear correlation with an increase in the

dx.doi.org/10.1021/bi300545f | Biochemistry 2012, 51, 7569−7579

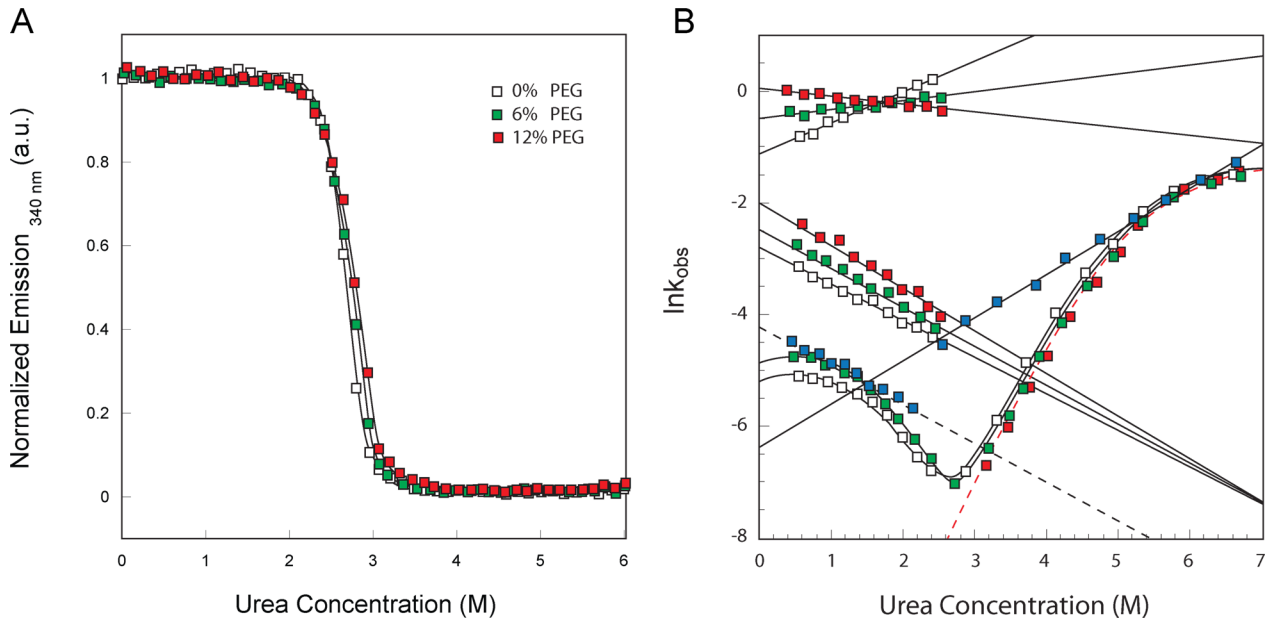

Figure 6. Assessment of the LacI folding landscape in the presence of a crowding agent. (A) Equilibrium unfolding of the LacI dimer at 1.5 μM protein in 6% PEG (green squares) and 12% PEG (red squares). (B) Observed kinetics of unfolding and folding as a function of the final urea concentration in 6% PEG (green squares) and 12% PEG (red squares). Results of FRET experiments in the presence of 6% PEG are shown as solid blues squares; results of FRET experiments at 12% PEG are listed in Table 3.

denaturant concentration, whereas the refolding reaction is composed of a fast relaxation phase that exhibits a positive slope, followed by a canonical linear dependence with an increase in urea concentration. Both transitions are observed using CD and fluorescence (see Figure S3 of the Supporting Information). However, the slowest kinetic phase is observed only by fluorescence; unlike the dimer, this phase has a linear dependence on urea concentration and is devoid of an apparent dependence on protein concentration. The putative four-phase folding mechanism for the tetramer shares features with both the monomer and the dimer:

$$U_4 \xrightarrow{k_{burst}} I_{Tb} \xrightarrow{k_1} I_{T1} \xrightarrow{k_2} I_{T2} \xrightarrow{k_3} N_4$$

though the unfolded tetramer (U_4) remains tethered by the C-terminal tetramerization domain.[14] The refolding reaction is initiated by a burst phase (I_{Tb}), followed by an observable reorganization event to form the first on-pathway intermediate (I_{T1}). The $I_{Tb} \rightarrow I_{T1}$ transition is similar to the $I_b \rightarrow I_{M1}$ transition for the dimer and the $I_b \rightarrow I$ transition for the monomer, though slightly faster. Accordingly, I_{T1} likely shares a similar conformation; i.e., the C-subdomain is mostly folded, whereas the N-subdomain is unfolded. The third reaction phase ($I_{T1} \rightarrow I_{T2}$) completes the formation of the (tethered) monomers, and this is followed by a minor reorganization ($I_{T2} \rightarrow N_4$) analogous to the $I_{M2} \rightarrow N_2$ transition. Notably, the $I_{T2} \rightarrow N_4$ transition does not require an explicit assembly because of tethering of the monomers via the tetramerization domain. The absence of a measurable FRET signal supports monomer preassembly, which is consistent with an earlier study.[14] Interestingly, tetramerization confers a 10-fold increase in the rate of formation of the native state when compared to that of the dimer reaction.

LacI Tetramer with a Perturbed Monomer−Monomer Interface. Two modifications to the LacI tetramer result in the production of a monomer: (i) a truncation of the last 11 residues from the tetramerization domain and (ii) and an L251A point mutation that perturbs the monomer−monomer interface.[1,12] Interestingly, the LacI tetramer with an L251A point mutation still results in a functional protein, capable of modulated DNA binding.[1,31] Here we evaluate the folding landscape of the L251A tetramer ($L251A_{tet}$) to gain confidence in the $I_{T2} \rightarrow N_4$ assignment, as this phase cannot be resolved by FRET experiments because of the surprisingly strong interaction conferred by the tetramerization domain.[14] Equilibrium unfolding experiments show that the L251A perturbation results in a shift in the unfolding midpoint to 2.4 M urea in addition to a reduction in the slope (16.1 kJ mol^{-1} M^{-1}); consequently, the stability is reduced by 26.8 kJ mol^{-1} (Figure 5A; data summarized in Table 2; also see Figure S3 of the Supporting Information). $L251A_{tet}$ folding dynamics are analogous to those of the LacI tetramer, where unfolding is an apparent single-phase reaction and refolding consists of four kinetic phases (also see Figure 5C):

$$U_{4,L251A} \xrightarrow{k_{burst}} I_{Tb} \xrightarrow{k_1} I_{T1} \xrightarrow{k_2} I_{T2} \xrightarrow{k_3} N_{4,L251A}$$

The key differences involve the rates of formation; namely, $L251A_{tet}$ has an extrapolated rate of unfolding that is 5 orders of magnitude faster than that of $LacI_{tet}$. In addition, reactions $I_{Tb} \rightarrow I_{T1}$ and $I_{T1} \rightarrow I_{T2}$ are slower, while the $I_{T2} \rightarrow N_{4,L251A}$ reaction is slightly faster and nearly convergent with the $I_{T1} \rightarrow I_{T2}$ transition.

LacI Folding Mechanism in the Presence of a Crowding Agent. Experimental and theoretical results[32−36] indicate that volume exclusion arising from the presence of background macromolecules (i.e., crowding agents) can profoundly influence the kinetics and equilibria of elementary isomerization and association reactions involved in protein folding and assembly.[32,33] In general, crowding affects equilibria by preferentially destabilizing reactants or products, such that the most favored state of the system excludes the least volume from the other macromolecular species present in solution.[32] To demonstrate that the proposed folding mechanisms for the

dx.doi.org/10.1021/bi300545f | Biochemistry 2012, 51, 7569−7579

Table 3. Equilibrium Unfolding and Dynamics of Unfolding and Folding of LacI in PEG[a]

	LacI dimer (1.5 μM) with 6% PEG		LacI dimer (1.5 μM) with 12% PEG		LacI tetramer (1.5 μM) with 12% PEG	
	fluorescence	far-UV CD	fluorescence	far-UV CD	fluorescence	far-UV CD
ΔG_{eq} (kJ mol^{-1})	45.7 ± 1.0	41.9 ± 1.2	42.3 ± 1.3	34.3 ± 1.4	64.1 ± 1.2	63.9 ± 2.0
m_{eq} (kJ mol^{-1} M^{-1})	16.9 ± 1.1	15.5 ± 1.5	15.1 ± 1.5	12.3 ± 2.0	22.1 ± 1.1	22.0 ± 1.5
$[urea]_{1/2eq}$ (M)	2.7 ± 0.1	2.7 ± 0.2	2.8 ± 0.1	2.8 ± 0.2	2.9 ± 0.1	2.9 ± 0.1
k_{burst} (s^{-1})	>1000	>1000	>1000	>1000	>1000	>1000
k_{f1} (s^{-1})	0.61 ± 0.03	0.59 ± 0.05	1.10 ± 0.05	0.99 ± 0.08	0.51 ± 0.02	0.50 ± 0.05
k_{f2} (s^{-1})	0.082 ± 0.002	0.083 ± 0.004	0.14 ± 0.01	0.17 ± 0.03	0.082 ± 0.002	0.079 ± 0.006
k_{f3} (s^{-1})	0.0034 ± 0.0003	–	–	–	0.045 ± 0.003	0.043 ± 0.008
k_u (s^{-1})	(5.1 ± 0.2) × 10^{-9}	(4.9 ± 0.3) ×10^{-9}	(2.3 ± 0.4) × 10^{-9}	(2.5 ± 0.6) ×10^{-9}	(5.9 ± 0.3) × 10^{-9}	(6.1 ± 0.5) × 10^{-9}
k_{f_FRET} (s^{-1})	0.014 ± 0.002	–	0.018 ± 0.001	–	–	–
k_{u_FRET} (s^{-1})	0.0017 ± 0.003	–	0.0012 ± 0.002	–	–	–

[a]Standard deviations are based on three or more independent experiments.

LacI dimer and tetramer are not simply the result of inert molecular crowding, we evaluated the folding landscape of the LacI dimer and tetramer in the presence of the crowding agent PEG. In other words, we conducted crowding studies (i) to illustrate the role of LacI monomer constituents as active reactants and (ii) to implicate the tetramerization domain as a unique constraint on the conformational space. A second critical benefit of this study is that it allows for a better understanding of how the cellular milieu (general crowding) may influence LacI dimer protein folding.

Equilibrium unfolding of the dimer at 1.5 μM protein in 6 and 12% PEG resulted in a change in the slope of the transition with a minor shift in the unfolding midpoint. Accordingly, protein stability is affected, resulting in an ∼6 kJ mol^{-1} decrease in the extrapolated stability, i.e., LacI dimer at 1.5 μM in the absence of PEG relative to the same protein concentration in 12% PEG (Figure 6A; data summarized in Table 3). Analysis of protein folding kinetics in the presence of PEG resulted in unfolding and refolding mechanisms similar to that observed for the dimer, with a few key differences (Figure 6B). First, the extrapolated rate of unfolding slows with an increase in PEG concentration. Interestingly, in the refolding reaction, the initial observed $I_b \rightarrow I_{M1}$ transition exhibits an increase in rate with a change in slope (positive to negative) with an increase in PEG concentration. The subsequent $I_{M1} \rightarrow I_{M2}$ transition also shows an increase in rate with an increase in PEG concentration, though with a canonical linear dependence with urea in all cases. Finally, the $I_{M2} \rightarrow N_2$ transition is observed at only 6% PEG and manifests with a slight increase in the rate (data summarized in Table 3). The change in slope with PEG concentration observed in the initial $U \rightarrow I_{M1}$ transition can be attributed to alterations in the burst-phase intermediate ($U \rightarrow {}^*I_b$) or changes in the unfolded state ($^*U \rightarrow I_b$) that restrict the structural ensemble of the unfolded state (or burst phase). The absence of the $I_{M2} \rightarrow N_2$ transition in the presence of 12% PEG can be attributed to the more nativelike structure of the $^*I_{M2}$ intermediate. Moreover, FRET experiments show a clearly distinct assembly phase in the presence of 6 and 12% PEG (Figure 6). Interestingly, the presence of PEG had little effect on tetramer folding (data summarized in Table 3). In general, the unfolding and folding of the LacI dimer in the presence of PEG are distinctly different from the observations for either the LacI dimer or tetramer in the absence of an inert crowding agent. While the reaction is still a four-phase folding mechanism, PEG appears to influence the conformational space of the unfolded and/or intermediate states, resulting in alterations of the folding mechanism.

SUMMARY

A better understanding of the folding landscapes of protein oligomers will provide key insights regarding the earliest stages of biological assembly, when proteins are most susceptible to aggregation and degradation. The folding mechanisms for the LacI dimer and tetramer presented here systematically build on our thorough understanding of the monomer folding landscape.[12,13] Whereas the LacI monomer is composed of three distinct phases, both oligomers include an additional reaction phase. The first three transitions of the LacI dimer and tetramer folding reactions are tantamount to monomer folding, though the rates of formation are faster, based on experimental unfolding and folding kinetics in which the first two observed reaction phases are approximately coincidental (see Figure 5B). However, the latter reaction phase for the dimer can be attributed to the assembly of mostly native monomers, based on curvature observed in the latter folding arm, where the protein is ∼100% folded via CD. This transition increases in rate with protein concentration and is devoid of protein aggregation. In addition, this reaction phase was explicitly assigned to protein assembly using intermolecular FRET experiments (see Figure 4). Similarly, the concluding reaction phase for LacI tetramer folding ($I_{T2} \rightarrow N_4$) can be attributed to an imposed intramolecular assembly of the monomers, accounting for the absence of any apparent concentration dependence, which is consistent with earlier equilibrium studies conducted by Matthews et al.[14] (also see Figure 5). The observations described above do not explicitly rule out the possibility of alternate folding routes; such pathways have been identified for the LacI monomer in silico. Accordingly, alternate pathways for LacI oligomers may be observed only via simulation,[12] which is beyond the scope of this study.

Evaluation of LacI dimer and tetramer folding in the presence of a molecular crowding agent clearly illustrates that the proposed mechanisms are not simply the result of intermolecular crowding; in addition, these data provide insight into the folding mechanism in vivo. The excluded volume effect[32,33,35,37] can have significant effects on the kinetics and thermodynamics of protein folding. While, the presence of the molecular crowding agent PEG results in a canonical increase in the rates of formation of the dimer product with a corresponding decrease in the extrapolated rate of unfolding, unexpectedly this does not result in additional stability (Figure 6). Interestingly, while a slight shift in the equilibrium midpoint is observed (Figure 6A), the presence of PEG results in a reduction in the slope of the unfolding transition (Table 3). In

addition, folding dynamics of the dimer reveal a distinct change in the rate and slope of the initial transition ($U \rightarrow I_{M1}$) (Figure 6B). Taken together, molecular crowding appears to influence the dimer folding reaction by restricting (or altering) the unfolded state ensemble (and/or the burst-phase intermediate). Interestingly, the LacI tetramer folding landscape is essentially unaffected by molecular crowding (under the conditions tested); this is likely due to the conformational restrictions imposed by the tetramerization domain, thus resulting in only modest changes in the extrapolated folding and unfolding rates. On the whole, the presence of PEG in dimer folding fails to recapitulate the folding mechanism of the dimer or tetramer. Rather, PEG shifts the dimer reaction to an alternate folding route, where the formation of folding intermediates and the native state is accelerated.

Theoretical and experimental studies have suggested that rugged energy landscapes will result in slower folding, where protein topology becomes the key determinant of the folding mechanism.[38−42] Moreover, the minimal frustration principle[39] can be extended and suggests that the protein's native topology is also the major factor that governs the choice of protein−protein assembly mechanisms.[43] Although robust theoretical frameworks are in place, derivation of detailed experimental descriptions of folding landscapes that include protein−protein assembly, which will allow us to test current theory, is significantly challenging. Several experimental studies that address both folding and protein assembly have been conducted;[9,25,44−47] however, few studies provide extensive detail regarding kinetic processes.[9,47] Accordingly, additional experimental landscapes are needed to improve predictive models for both protein folding and assembly. In this study, we show experimentally the (mechanistic) effects of oligomerization that involve large monomer constituents with complex topology. In brief, while dimerization does increase the complexity of the LacI folding reaction, tetramerization surprisingly decreased the complexity of the folding−assembly landscape via elimination of explicit monomer association in the latter reaction phase.

The folding mechanism for proteins that share the same topology with LacI can presumably have similar folding mechanisms;[38−42] however, divergences can also occur because of permutation in the main chain connectivity and/or amino acid composition. In one case, circular permutants should represent a series of proteins that do not vary in their amino acid composition, structure, or type of enthalpic interaction stabilizing the protein. Hence, circular permutation has been used to examine the role of topology in protein folding rates and mechanisms.[48] Circular permutation of ribosomal protein S6 as shown by Oliveberg et al.[49] can change the preferred folding route and the structure of the folding nucleus. Accordingly, natural permutation as well as differences in amino acid composition in the family of proteins that share LacI's topology will likely influence both the folding and assembly mechanisms. Thus, predictive models of folding mechanisms of large proteins with complex topology that assemble will require reconciliation of both main chain permutation and composition.

While considerable efforts have focused on reconciling protein−protein complexes in the ground (native) state,[50] relatively few studies with a goal of understanding the folding mechanisms of protein dimers and higher-order oligomers have been conducted. Deciphering the dynamic principles of complex protein association is crucial for the understanding of protein function and misfolding. An improved understanding of topologically complex protein assembly in the earliest stages will allow the design of novel protein−protein interactions, as the principles of non-two-state protein folding of oligomers are not adequately represented in current computational design algorithms.[51,52] Protein design studies that incorporate mechanistic details of protein folding and assembly are currently underway.

■ ASSOCIATED CONTENT

Ⓢ Supporting Information

Protein expression and purification information, protein folding−assembly dynamics and analysis, and ligand analogue binding data obtained by isothermal titration calorimetry. This material is available free of charge via the Internet at http://pubs.acs.org.

■ AUTHOR INFORMATION

Corresponding Author

*Department of Chemical and Environmental Engineering and Department of Molecular Biophysics and Biochemistry, Yale University, 55 Prospect St., Malone Engineering Center 214, New Haven, CT 06511. Telephone: (203) 432-9888. Fax: (203) 436-4861. E-mail: corey.wilson@yale.edu.

Funding

This work was supported by National Science Foundation Grant 1133834, awarded to C.J.W.

Notes

The authors declare no competing financial interest.

■ ACKNOWLEDGMENTS

We thank Dr. Stanley Howell for reviewing this article and providing critical comments and suggestions.

■ REFERENCES

(1) Dong, F. M., Spott, S., Zimmermann, O., Kisters-Woike, B., Muller-Hill, B., and Barker, A. (1999) Dimerisation mutants of Lac repressor. I. A monomeric mutant, L251A, that binds lac operator DNA as a dimer. *J. Mol. Biol. 290*, 653−666.

(2) Anderson, W. F., Ohlendorf, D. H., Takeda, Y., and Matthews, B. W. (1981) Structure of the cro repressor from bacteriophage λ and its interaction with DNA. *Nature 290*, 754−758.

(3) Pabo, C. O., and Lewis, M. (1982) The operator-binding domain of λ repressor: Structure and DNA recognition. *Nature 298*, 443−447.

(4) Pavletich, N. P., and Pabo, C. O. (1991) Zinc finger-DNA recognition: Crystal structure of a Zif268-DNA complex at 2.1 Å. *Science 252*, 809−817.

(5) Konig, P., and Richmond, T. J. (1993) The X-ray structure of the GCN4-bZIP bound to ATF/CREB site DNA shows the complex depends on DNA flexibility. *J. Mol. Biol. 233*, 139−154.

(6) Somers, W. S., and Phillips, S. E. (1992) Crystal structure of the met repressor-operator complex at 2.8 Å resolution reveals DNA recognition by β-strands. *Nature 359*, 387−393.

(7) Ohlendorf, D. H., Anderson, W. F., Fisher, R. G., Takeda, Y., and Matthews, B. W. (1982) The molecular basis of DNA-protein recognition inferred from the structure of cro repressor. *Nature 298*, 718−723.

(8) Sauer, R. T., Yocum, R. R., Doolittle, R. F., Lewis, M., and Pabo, C. O. (1982) Homology among DNA-binding proteins suggests use of a conserved super-secondary structure. *Nature 298*, 447−451.

(9) Rumfeldt, J. A. O., Galvagnion, C., Vassall, K. A., and Meiering, E. M. (2008) Conformational stability and folding mechanisms of dimeric proteins. *Prog. Biophys. Mol. Biol. 98*, 61−84.

(10) Wilson, C. J., Zhan, H., Swint-Kruse, L., and Matthews, K. S. (2007) The lactose repressor system: Paradigms for regulation, allosteric behavior and protein folding. *Cell. Mol. Life Sci. 64*, 3−16.
(11) Rutkauskas, D., Zhan, H. L., Matthews, K. S., Pavone, F. S., and Vanzi, F. (2009) Tetramer opening in LacI-mediated DNA looping. *Proc. Natl. Acad. Sci. U.S.A. 106*, 16627−16632.
(12) Das, P., Wilson, C. J., Fossati, G., Wittung-Stafshede, P., Matthews, K. S., and Clementi, C. (2005) Characterization of the folding landscape of monomeric lactose repressor: Quantitative comparison of theory and experiment. *Proc. Natl. Acad. Sci. U.S.A. 102*, 14569−14574.
(13) Wilson, C. J., Das, P., Clementi, C., Matthews, K. S., and Wittung-Stafshede, P. (2005) The experimental folding landscape of monomeric lactose repressor, a large two-domain protein, involves two kinetic intermediates. *Proc. Natl. Acad. Sci. U.S.A. 102*, 14563−14568.
(14) Barry, J. K., and Matthews, K. S. (1999) Thermodynamic analysis of unfolding and dissociation in lactose repressor protein. *Biochemistry 38*, 6520−6528.
(15) Chen, J., and Matthews, K. S. (1994) Subunit Dissociation Affects DNA-Binding in a Dimeric Lac Repressor Produced by C-Terminal Deletion. *Biochemistry 33*, 8728−8735.
(16) Wilson, C. J., Zhan, H. L., Swint-Kruse, L., and Matthews, K. S. (2007) Ligand interactions with lactose repressor protein and the repressor-operator complex: The effects of ionization and oligomerization on binding. *Biophys. Chem. 126*, 94−105.
(17) Chen, J., and Matthews, K. S. (1992) Deletion of Lactose Repressor Carboxyl-Terminal Domain Affects Tetramer Formation. *J. Biol. Chem. 267*, 13843−13850.
(18) Lowry, O. H., Rosebrough, N. J., Farr, A. L., and Randall, R. J. (1951) Protein measurement with the Folin phenol reagent. *J. Biol. Chem. 193*, 265−275.
(19) Santoro, M. M., and Bolen, D. W. (1988) Unfolding Free-Energy Changes Determined by the Linear Extrapolation Method. 1. Unfolding of Phenylmethanesulfonyl α-Chymotrypsin Using Different Denaturants. *Biochemistry 27*, 8063−8068.
(20) Fersht, A. R. (1997) Nucleation mechanisms in protein folding. *Curr. Opin. Struct. Biol. 7*, 3−9.
(21) Otzen, D. E., Kristensen, O., Proctor, M., and Oliveberg, M. (1999) Structural changes in the transition state of protein folding: alternative interpretations of curved chevron plots. *Biochemistry 38*, 6499−6511.
(22) Ternstrom, T., Mayor, U., Akke, M., and Oliveberg, M. (1999) From snapshot to movie: ϕ analysis of protein folding transition states taken one step further. *Proc. Natl. Acad. Sci. U.S.A. 96*, 14854−14859.
(23) Pace, C. N., and Shaw, K. L. (2000) Linear extrapolation method of analyzing solvent denaturation curves. *Proteins,*, 1−7.
(24) Soulages, J. L. (1998) Chemical denaturation: Potential impact of undetected intermediates in the free energy of unfolding and m-values obtained from a two-state assumption. *Biophys. J. 75*, 484−492.
(25) Mallam, A. L., and Jackson, S. E. (2007) A comparison of the folding of two knotted proteins: YbeA and YibK. *J. Mol. Biol. 366*, 650−665.
(26) Hobart, S. A., Meinhold, D. W., Osuna, R., and Colon, W. (2002) From two-state to three-state: The effect of the P61A mutation on the dynamics and stability of the factor for inversion stimulation results in an altered equilibrium denaturation mechanism. *Biochemistry 41*, 13744−13754.
(27) Mallam, A. L., and Jackson, S. E. (2005) Folding studies on a knotted protein. *J. Mol. Biol. 346*, 1409−1421.
(28) Sanchez, I. E., and Kiefhaber, T. (2003) Hammond behavior versus ground state effects in protein folding: Evidence for narrow free energy barriers and residual structure in unfolded states. *J. Mol. Biol. 327*, 867−884.
(29) Sanchez, I. E., and Kiefhaber, T. (2003) Non-linear rate-equilibrium free energy relationships and Hammond behavior in protein folding. *Biophys. Chem. 100*, 397−407.
(30) Sanchez, I. E., and Kiefhaber, T. (2003) Evidence for sequential barriers and obligatory intermediates in apparent two-state protein folding. *J. Mol. Biol. 325*, 367−376.
(31) Suckow, J., Markiewicz, P., Kleina, L. G., Miller, J., KistersWoike, B., and MullerHill, B. (1996) Genetic studies of the Lac repressor. 15. 4000 single amino acid substitutions and analysis of the resulting phenotypes on the basis of the protein structure. *J. Mol. Biol. 261*, 509−523.
(32) Minton, A. P. (2000) Implications of macromolecular crowding for protein assembly. *Curr. Opin. Struct. Biol. 10*, 34−39.
(33) Minton, A. P. (2005) Influence of macromolecular crowding upon the stability and state of association of proteins: Predictions and observations. *J. Pharm. Sci. 94*, 1668−1675.
(34) Samiotakis, A., Wittung-Stafshede, P., and Cheung, M. S. (2009) Folding, Stability and Shape of Proteins in Crowded Environments: Experimental and Computational Approaches. *Int. J. Mol. Sci. 10*, 572−588.
(35) van den Berg, B., Ellis, R. J., and Dobson, C. M. (1999) Effects of macromolecular crowding on protein folding and aggregation. *EMBO J. 18*, 6927−6933.
(36) Samiotakis, A., and Cheung, M. S. (2011) Folding dynamics of Trp-cage in the presence of chemical interference and macromolecular crowding. I. *J. Chem. Phys. 135*, 175101.
(37) Ai, X. J., Zhou, Z., Bai, Y. W., and Choy, W. Y. (2006) ^{15}N NMR spin relaxation dispersion study of the molecular crowding effects on protein folding under native conditions. *J. Am. Chem. Soc. 128*, 3916−3917.
(38) Baker, D. (2000) A surprising simplicity to protein folding. *Nature 405*, 39−42.
(39) Onuchic, J. N., Socci, N. D., LutheySchulten, Z., and Wolynes, P. G. (1996) Protein folding funnels: The nature of the transition state ensemble. *Folding Des. 1*, 441−450.
(40) Clementi, C., Nymeyer, H., and Onuchic, J. N. (2000) Topological and energetic factors: What determines the structural details of the transition state ensemble and "en-route" intermediates for protein folding? An investigation for small globular proteins. *J. Mol. Biol. 298*, 937−953.
(41) Wensley, B. G., Batey, S., Bone, F. A. C., Chan, Z. M., Tumelty, N. R., Steward, A., Kwa, L. G., Borgia, A., and Clarke, J. (2010) Experimental evidence for a frustrated energy landscape in a three-helix-bundle protein family. *Nature 463*, 685−688.
(42) Steward, A., McDowell, G. S., and Clarke, J. (2009) Topology is the Principal Determinant in the Folding of a Complex All-α Greek Key Death Domain from Human FADD. *J. Mol. Biol. 389*, 425−437.
(43) Levy, Y., Wolynes, P. G., and Onuchic, J. N. (2004) Protein topology determines binding mechanism. *Proc. Natl. Acad. Sci. U.S.A. 101*, 511−516.
(44) Clark, A. C., Raso, S. W., Sinclair, J. F., Ziegler, M. M., Chaffotte, A. F., and Baldwin, T. O. (1997) Kinetic mechanism of luciferase subunit folding and assembly. *Biochemistry 36*, 1891−1899.
(45) Svensson, A. K. E., Bilsel, O., Kondrashkina, E., Zitzewitz, J. A., and Matthews, C. R. (2006) Mapping the folding free energy surface for metal-free human Cu,Zn superoxide dismutase. *J. Mol. Biol. 364*, 1084−1102.
(46) Doyle, S. M., Braswell, E. H., and Teschke, C. M. (2000) SecA folds via a dimeric intermediate. *Biochemistry 39*, 11667−11676.
(47) Mateu, M. G., Del Pino, M. M. S., and Fersht, A. R. (1999) Mechanism of folding and assembly of a small tetrameric protein domain from tumor suppressor p53. *Nat. Struct. Biol. 6*, 191−198.
(48) Miller, E. J., Fischer, K. F., and Marqusee, S. (2002) Experimental evaluation of topological parameters determining protein-folding rates. *Proc. Natl. Acad. Sci. U.S.A. 99*, 10359−10363.
(49) Haglund, E., Lindberg, M. O., and Oliveberg, M. (2008) Changes of protein folding pathways by circular permutation: Overlapping nuclei promote global cooperativity. *J. Biol. Chem. 283*, 27904−27915.
(50) Perrakis, A., Musacchio, A., Cusack, S., and Petosa, C. (2011) Investigating a macromolecular complex: The toolkit of methods. *J. Struct. Biol. 175*, 106−112.
(51) Leaver-Fay, A., Tyka, M., Lewis, S. M., Lange, O. F., Thompson, J., Jacak, R., Kaufman, K., Renfrew, P. D., Smith, C. A., Sheffler, W., Davis, I. W., Cooper, S., Treuille, A., Mandell, D. J., Richter, F., Ban, Y.

E. A., Fleishman, S. J., Corn, J. E., Kim, D. E., Lyskov, S., Berrondo, M., Mentzer, S., Popovic, Z., Havranek, J. J., Karanicolas, J., Das, R., Meiler, J., Kortemme, T., Gray, J. J., Kuhlman, B., Baker, D., and Bradley, P. (2011) Rosetta3: An Object-Oriented Software Suite for the Simulation and Design of Macromolecules. *Methods Enzymol. 487*, 545−574.

(52) Alvizo, O., Allen, B. D., and Mayo, S. L. (2007) Computational protein design promises to revolutionize protein engineering. *BioTechniques 42*, 31−39.